Proceedings of the 10th WSEAS International Conference on CIRCUITS, Vouliagmeni, Athens, Greece, July 10-12, 2006 (pp330-335)

Comparison of the DR of continuous time G_m-C filters using different structures

J. FRANCISCO FERNÁNDEZ-BOOTELLO, MANUEL. DELGADO-RESTITUTO, A. RODRÍGUEZ VÁZQUEZ, DAVIDE BRANDANO
Instituto de Microelectónica de Sevilla, Centro Nacional de Microelectrónica
Avda. Reina Mercedes s/n, 41012-Sevilla (España), Tel: +34 - 95 505 6666

Abstract: This paper presents design techniques to evaluate the noise and distortion of continuous time Gm-C filters. Also presents techniques to improve the dynamic range of such filters keeping a relation of integer numbers between the transconductors. Furthermore the comparison of the dynamic range for the same power using different structures is presented**.**

Key Words: Continuous time filters, low noise, high linearity, G_m-C filters, Volterra's series, analog circuits, lc ladder.

1. Introduction†

G_m-C filters are widely used in many applications as communications systems, hard disk drivers and instrumentation [1]. There are many factors which can degrade the behaviour of such filters. One key figure of merit which measures such degradation is the dynamic range (**DR**) of the circuit, which can be defined as the ratio among the maximum signal power level (for a given distortion at the output) which can be processed by the filter and the total integrated noise power. This DR can hardly depend on the structure used to implement the filter, so the choice of the structure can be crucial for the designer. It can be demonstrated that the DR is directly related with the power consumption of the filter [2]. Thus the DR for a constant power is a good figure of merit to compare different structures. In this paper we will compare the DR of three commonly used structures: Cascade connections of biquadratic sections[1],[3], LC ladder simulations[2],[4] and the inverse follow the leader structure (**FLF**) [1],[5]. To make that comparison we need techniques to evaluate the noise and distortion of the filter in a fast way. Here we proposed a fast way to evaluate the noise and distortion of continuous time filters using matrices. In particular the distortion is achieved using Volterra's series theory [7] which avoid the use of lengthy transient analysis. This fact allows us to use an optimization process to improve the characteristics of the filters. The paper is structured as follow. Sec. 2 shows a method to describe filters using a dot matrix notation. Using that notation, the noise and distortion can be easily described (Sec. 3-Sec. 4). In Sec. 5 we explain how by changing the internal nodes magnitude and the total impedance associated to one node the distortion and noise can be modified. Also a method to scale the filter using unitary transconductors is presented. Sec. 6 shows a comparison of the three structures mentioned above using a seventh order, low-pass Chebyshev filter and finally Sec. 7 shows the conclusions.

†.**Acknowledgement**: This work has been partially funded by the spanish MCyT under Project TIC2003-02355 (RAICONIF).

2. Space state representation

G_m-C filters can be described using an extended state-space notation as follow [1],

$$\begin{aligned} s\mathbf{E}\mathbf{x} &= \mathbf{A}\mathbf{x} + \mathbf{B}v_I \\ v_O &= \mathbf{C}\mathbf{x} + Dv_I \end{aligned} \tag{1}$$

where v_I and v_O are, respectively, the input and output voltages of the filter; $\mathbf{x} = [x_1, \ldots, x_n]^\dagger$ is a state vector which gathers all the n internal node voltages together; $\mathbf{A}$ is an $n \times n$ matrix whose element a_{ij} represents the gain of the transconductor connected from node x_j (input) to x_i (output) for $i, j = 1, \ldots, n$; $\mathbf{B}$ is an $n \times 1$ vector given by,

$$\mathbf{B} = \mathbf{B}_G + s\mathbf{B}_C = [b_1 + sC_{b1}, \ldots, b_n + sC_{bn}]^\dagger \tag{2}$$

where b_i and C_{bi} represent, respectively, the transconductance and capacitance between the filter input and integration node x_i – $\mathbf{B}_G$ is formed by transconductances and $\mathbf{B}_C$ is composed by capacitances. $\mathbf{C}$ is a $1 \times n$ vector whose element c_j denotes the voltage amplification provided by a transconductor with input x_j and gain $g_o c_j$, loaded with a resistor of resistance $1/g_o$. Similarly, D is a scalar which represents the voltage amplification of a transconductor with input v_I and gain $g_o d$ loaded by the same unity-gain feedback output transconductor. Most often, the output of the filter is taken from a single internal node, configuration for which $\mathbf{C}$ becomes multiple of a unit vector, i.e., $C = [0, \ldots, c_j, \ldots, 0]$, and $D = 0$. Moreover, if no output voltage amplification is required, then vector $\mathbf{C}$ is unitary and the output summing network can be suppressed. Finally, $\mathbf{E}$ is an $n \times n$ matrix composed by capacitances where e_{ij} represent a capacitor which goes from the node *i* to the node *j*.

From the representation (1), the input-output transfer function of the filter can be easily calculated as

$$H(s) = \frac{v_O}{v_I} = \mathbf{C}(s\mathbf{E} - \mathbf{A})^{-1}\mathbf{B} + D \tag{3}$$

For reasons that will become apparent in the following sections, it is worth defining other transfer functions. Let f_i be the transfer function from v_I to the integration node x_i. It can be easily shown that, denoting

$$\mathbf{F} = \left[f_1, f_2, \ldots, f_n\right]^{\dagger} \tag{4}$$

the following equation holds,

$$\mathbf{F} = (s\mathbf{E} - \mathbf{A})^{-1}\mathbf{B} \tag{5}$$

On the other hand, let g_i be the transfer function from a current source connected at integration node x_i (between the output terminals of transconductors with gain a_{ij} for $j = 1, \ldots, n$) to the filter output for $v_I = 0$. If all the transfer functions g_i, $i = 1, \ldots, n$, are collected in a vector

$$\mathbf{G} = \left[g_1\ g_2\ \ldots g_n\right] \tag{6}$$

it is easy to show that

$$\mathbf{G} = \mathbf{C}(s\mathbf{E} - \mathbf{A})^{-1} \tag{7}$$

3. Noise in G_m-C Filters

In this paper, it is assumed that capacitors are noiseless and, hence, that the only sources of noise in G_m-C filters are due to transconductors. Further, it is assumed that all noise sources are uncorrelated and that they are dominated by thermal contributions. With these hypothesis, the noise due a transconductor with gain G_m can be modelled by a current noise source between its output terminals with double-sided power spectral density (PSD) $2kT\xi G_m$ where k is Boltzmann´s constant, T is the absolute temperature, and ξ is the noise excess factor of the transconductor, which depends on its particular circuit-level implementation.

Using the above expression for the PSD, and the transfer functions g_i defined in the previous section, the total output-referred noise voltage PSD of the filter can be evaluated as

$$S_G(\omega) = 2kT\xi\sum_i |g_i(\omega)|^2\left(|b_i| + \sum_j |a_{ij}|\right) + \frac{2kT\xi}{g_o}\left(|d| + \sum_i |c_i|\right) \tag{8}$$

where the first sum accounts for the noise contributions of all the transconductors in the filter core, and the second sum corresponds to the presence of a non-trivial output summer. In the foregoing analysis it is assumed that the second term in (8) is negligible small as compared to the contributions from the filter core (this demands that the output transconductance g_o be high enough), or null, revealing the common-place situation in which the output of the filter is simply taken from a single internal node. With this assumption, the total output noise mean-squared value of the filter is approximately given by,

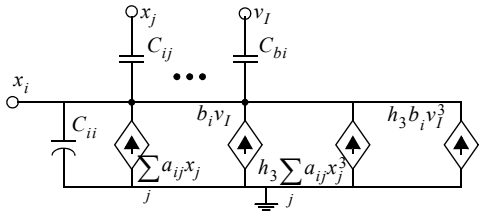

Fig. 1. Conceptual schematic at the i-th integration node of the filter including non-linearities.

$$\overline{U_{no}^2} \approx \frac{1}{2\pi}\int_{-\infty}^{\infty} S_G(\omega)d\omega \tag{9}$$

which can be regarded as an upper-limit value as it is assumed that the response of transconductors does not degrade with frequency. In order to evaluate the integral in (9) it is worth mentioning that the observability grammian matrix [4]

$$\mathbf{W} = \frac{1}{2\pi}\int_{-\infty}^{\infty} \mathbf{G}^{\dagger}(-j\omega)\mathbf{G}(j\omega)d\omega \tag{10}$$

can be algebraically obtained from the following Lyapunov equation [6]

$$\mathbf{E}^{\dagger}\mathbf{W}\mathbf{A} + \mathbf{A}^{\dagger}\mathbf{W}\mathbf{E} = -\mathbf{C}^{\dagger}\mathbf{C} \tag{11}$$

and, therefore, the total noise of the filter can be written as

$$\overline{U_{no}^2} = 2kT\xi\sum_i w_{ii}\left(|b_i| + \sum_j |a_{ij}|\right) = \sum_i \overline{U_{no,i}^2} \tag{12}$$

where w_{ii}, $i = 1, \ldots, n$, represent the elements at the diagonal of matrix $\mathbf{W}$, and $\overline{U_{no,i}^2}$ is the noise contributed to the output from the *i-th* integration node.

4. Distortion in G_m-C Filters

The main source of distortion in fully-differential G_m-C filters is the third-order harmonic component exhibited by transconductors. Hence, neglecting second-order (this is justified by the balanced structure of the transconductor) and high-order terms, the output current of the transconductor can be approximated as

$$i \approx G_{mo}v(1 + h_3 v^2) \tag{13}$$

where h_3 the third-order non linearity coefficient and v is the input voltage. Taking into account (13) the extended state-space representation in (1) becomes,

$$\begin{aligned} \mathbf{E}\frac{d\mathbf{x}}{dt} - \mathbf{B}_C\frac{dv_I}{dt} &= \mathbf{A}\mathbf{x} + h_3\mathbf{A}\mathbf{x}^{(3)} + \mathbf{B}_G v_I + h_3\mathbf{B}_G v_I^3 \\ v_O &= \mathbf{C}\mathbf{x} + Dv_I \end{aligned} \tag{14}$$

where $\mathbf{x}^{(3)} = \left[x_1^3, x_2^3, \ldots, x_n^3\right]^{\dagger}$ is the Hadamard cube† of $\mathbf{x}$.

Fig.1 shows a conceptual schematic of the i-th node of the filter, according to the representation (14).

†.The Hadamard product of two $m \times n$ matrices $\mathbf{A}$ and $\mathbf{B}$, denoted by $\mathbf{A} \bullet \mathbf{B}$, is an $m \times n$ matrix given by $(\mathbf{A} \bullet \mathbf{B})_{ij} = a_{ij}b_{ij}$.

Several approaches can be found in the literature for the analysis of the non-linear behaviour described by (14) [7]-[8]. The one herein proposed relies on Volterra's series expansions [7]. This method, suitable for weakly non-linear systems, consists on decomposing the internal nodes variables in operators, according to

$$\mathbf{x}(v_I(t)) = \mathbf{x}_1(v_I(t)) + \mathbf{x}_2(v_I(t)) + \ldots + \mathbf{x}_n(v_I(t)) = \sum_k \mathbf{x}_k(v_I(t)) \quad (15)$$

where

$$\mathbf{x}_k(v_I(t)) = \int_{-\infty}^{\infty} \ldots \int_{-\infty}^{\infty} \mathbf{h}_k(\tau_1 \ldots \tau_k) v_I(t-\tau_1) \ldots v_I(t-\tau_k) d\tau_1 \ldots d\tau_k \quad (16)$$

is referred to as the k-th order Volterra operator and $\mathbf{h}_k(.)$ is the k-th Volterra kernel [7]. The Laplace transform of this multidimensional kernel is defined as follows

$$\mathbf{H}_k(s_1, \ldots s_k) = \int_{-\infty}^{\infty} \ldots \int_{-\infty}^{\infty} \mathbf{h}_k(\tau_1 \ldots \tau_k) e^{-(s_1\tau_1 \ldots + s_k\tau_k)} d\tau_1 \ldots d\tau_k \quad (17)$$

where s_k is the k-dimensional Laplace variable. The relevant feature of Volterra's series expansions approach is that $\mathbf{H}_1(s_1)$ gives a formal description of the linear behaviour of the system in the frequency domain, whereas, $\mathbf{H}_3(s_1, s_2, s_3)$ does of the third-order non-linear behaviour, which is the only one considered in the approximation (13). Note from (15) and (16) that

$$\mathbf{x}(\rho v_I(t)) = \sum_k \rho^k \mathbf{x}_k(v_I(t)) \quad (18)$$

which is a power series in the amplitude scaling factor ρ [7]. For weakly non-linear systems and low values of ρ this series rapidly converges and can be approximated for the first few terms. Let us consider, in agreement with (13), that $\mathbf{x}(v_I) \approx \mathbf{x}_1(v_I) + \mathbf{x}_3(v_I)$ and, therefore, that equation (14) can be approximated as follows

$$\mathbf{E}\frac{d(\mathbf{x}(\rho v_I))}{dt} - \mathbf{B}_C\frac{\rho dv_I}{dt} \approx \mathbf{A}\mathbf{x}(\rho v_I) + h_3\mathbf{A}\mathbf{x}(\rho v_I)^{(3)} + \rho\mathbf{B}v_I + h_3\rho^3\mathbf{B}_G v_I^3 \quad (19)$$
$$v_O = \mathbf{C}\mathbf{x}(\rho v_I) + \rho D v_I = v_{O1} + v_{O3}$$

Grouping terms with the same power of ρ, (19) can be decomposed into the following two linear systems in $\mathbf{x}_1$ and $\mathbf{x}_3$

$$\begin{aligned} \mathbf{E}\dot{\mathbf{x}}_1 - \mathbf{B}_C\frac{dv_I}{dt} &= \mathbf{A}\mathbf{x}_1 + \mathbf{B}_G v_I \\ v_{O1} &= \mathbf{C}\mathbf{x}_1 + D v_I \end{aligned} \quad (20)$$

and

$$\begin{aligned} \mathbf{E}\dot{\mathbf{x}}_3 &= \mathbf{A}\mathbf{x}_3 + h_3(\mathbf{A}\mathbf{x}_1^3 + \mathbf{B}_G v_I^3) \\ v_{O3} &= \mathbf{C}\mathbf{x}_3 \end{aligned} \quad (21)$$

which can be mapped into the first- and third-order circuits shown in Fig. 2(a) and (b), respectively. Solving both circuits, the first- and third-order transformed kernels of the filter are respectively given by

$$\mathbf{H}_1(s_1) = \frac{\mathbf{x}_1}{v_I} = (\mathbf{E}s_1 - \mathbf{A})^{-1}\mathbf{B} \quad (22)$$

and

$$\mathbf{H}_3(s_1, s_2, s_3) = \frac{\mathbf{x}_3}{v_I} = h_3(\mathbf{E}(s_1+s_2+s_3) - \mathbf{A})^{-1} \quad (23)$$
$$(\mathbf{A}\mathbf{H}_1(s_1) \bullet \mathbf{H}_1(s_2) \bullet \mathbf{H}_1(s_3) + \mathbf{B}_G)$$

from where, the third-order harmonic distortion of the filter and its inter-modulation performance can be estimated, with no need of transient analysis, by [7]

$$\begin{aligned} HD_3(\omega) &= \frac{1}{4}\left|\frac{\mathbf{C}\mathbf{H}_3(j\omega, j\omega, j\omega)}{\mathbf{C}\mathbf{H}_1(j\omega)}\right|\rho^2 \\ IM_3(2\omega_1 \pm \omega_2) &= \frac{3}{4}\left|\frac{\mathbf{C}\mathbf{H}_3(j\omega_1, j\omega_1, \pm j\omega_2)}{\mathbf{C}\mathbf{H}_1(j\omega_1)}\right|\rho^2 \end{aligned} \quad (24)$$

where ρ is the amplitude of the input tones applied to the system. Obviously, the lower ρ, the lower the distortion generated by the system.

Equation (24) can be related to matrices $\mathbf{F}$ and $\mathbf{G}$, defined in Sec. 2, as follows

$$\begin{aligned} HD_3(\omega) &= \frac{1}{4}\left|\frac{\mathbf{G}(3\omega)(\mathbf{A}\mathbf{F}^{(3)}(\omega) + \mathbf{B}_G)}{H(\omega)}\right|\rho^2 \\ IM_3(2\omega_1 \pm \omega_2) &= \frac{3}{4}\left|\frac{\mathbf{G}(2\omega_1 \pm \omega_2)(\mathbf{A}\mathbf{F}(\omega_1) \bullet \mathbf{F}(\pm\omega_2) + \mathbf{B}_G)}{H(\omega)}\right|\rho^2 \end{aligned} \quad (25)$$

which reveals that the distortion evaluation of a G_m-C filter can be easily accomplished by simple matrix algebra. Analogous expressions to (25) have been also reported in [8].

5. Scaling of *Gm-C* filters

From a mathematical point of view, filter scaling implies transforming the matrices which describe the system, so that some of the filter properties become altered with respect to the original prototype. In the following, if x denotes a given variable in the prototype system, $\tilde{x}$ represents the corresponding transformed variable.

In this section, only those scaling operations which retain the input-output transfer function of the un-scaled filter $H(s)$ will be considered†,furthermore the influence of scaling on the noise and distortion performance of the filter will be discussed.

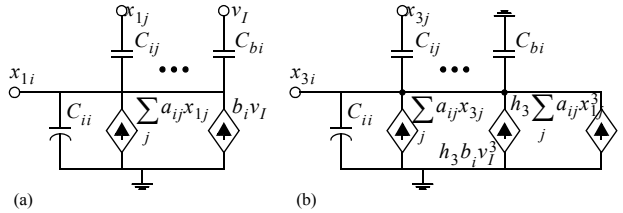

Fig. 2. (a) First order circuit at node x_i, (b) Third order circuit at node x_i

†.This excludes frequency scaling operations which are easily implemented by multiplying all the filter capacitances by the same factor α_C (this makes $\tilde{\mathbf{E}} = \alpha_C\mathbf{E}$ and $\tilde{\mathbf{B}}_C = \alpha_C\mathbf{B}_C$ and, thereafter, $\tilde{H}(s) = H(\alpha_C s)$) or by concurrently scaling all the filter transconductances by α_G (this makes $\tilde{\mathbf{A}} = \alpha_G\mathbf{A}$ and $\tilde{\mathbf{B}}_G = \alpha_G\mathbf{B}_G$ and, thereafter, $\tilde{H}(s) = H(s/\alpha_G)$).

A first approach for filter scaling consists on multiplying each row of the state equation in (1) by a corresponding positive number. Recasting all these factors, β_i for $i = 1, \ldots, n$, into a diagonal matrix $\mathbf{Diag}(\{\beta_i\})$, this kind of scaling implies the following transformations,

$$\begin{aligned} \tilde{\mathbf{E}} &= \mathbf{Diag}(\{\beta_i\})\mathbf{E} \\ \tilde{\mathbf{A}} &= \mathbf{Diag}(\{\beta_i\})\mathbf{A} \\ \tilde{\mathbf{B}} &= \mathbf{Diag}(\{\beta_i\})\mathbf{B} \end{aligned} \tag{26}$$

whose impact on the transfer functions defined in Section 2 can be demonstrated to be,

$$\begin{aligned} \tilde{\mathbf{F}} &= (s\tilde{\mathbf{E}} - \tilde{\mathbf{A}})^{-1}\tilde{\mathbf{B}} = \mathbf{F} \\ \tilde{\mathbf{G}} &= \mathbf{C}(s\tilde{\mathbf{E}} - \tilde{\mathbf{A}})^{-1} = \mathbf{G}\mathbf{Diag}(\{1/\beta_i\}) \end{aligned} \tag{27}$$

from where the identity $\tilde{H}(s) = H(s)$ can be easily derived. From (27), it can be deduced that the transformation in (26) introduces local impedance scaling at each node of the filter, but does not alter their voltage swings. Hence, this transformation does not affect the distortion behaviour of the filter, as can be easily demonstrated by replacing (26) and (27) into (25). On the other hand, taking into account the definition of the grammian matrix $\mathbf{W}$ in (10), it can be found that

$$\tilde{w}_{ii} = w_{ii}\left(\frac{1}{\beta_i^2}\right) \tag{28}$$

and considering that the sum of all the transconductances driving the *i*-th node of the filter is given by $\tilde{G}_i = |\tilde{b}_i| + \sum_{j=1,\ldots,n} |\tilde{a}_{ij}| = \beta_i G_i$, then the noise contributed to the output from the *i-th* integration node in the scaled filter becomes,

$$\overline{\tilde{U}^2_{no,i}} = \frac{1}{\beta_i}\overline{U^2_{no,i}} \tag{29}$$

and, therefore, the transformation (26) can be interpreted as a form of *noise scaling*. Note that reducing the noise contribution at node *i* by a factor $\beta_i > 1$ implies increasing the total transconductance G_i by the same factor, thus rising the power consumption of the filter. Additionally, the area occupation also increases as the required capacitances are scaled by β_i.

It is interesting to recast (29) into the following form

$$\overline{\tilde{U}^2_{no,i}} = \frac{\kappa_i}{\tilde{G}_i} \tag{30}$$

where $\kappa_i = G_i\overline{U^2_{no,i}}$, for $i = 1, \ldots, n$, are parameters that only depend on the prototype filter (they are not affected by noise scaling) and, therefore, they do not depend on the total transconductance driving the *i*-th node. This is an important result as it allows to determine the optimum noise scaling factor for a given total filter transconductance $G_{tot} = \sum_{i=1,\ldots,n} \tilde{G}_i$ by making [2], [8]

$$\frac{\kappa_1}{\tilde{G}_1^2} = \frac{\kappa_2}{\tilde{G}_2^2} = \ldots = \frac{\kappa_n}{\tilde{G}_n^2} \tag{31}$$

what gives

$$\tilde{G}_i = \frac{\sqrt{\kappa_i}}{\sum_i \sqrt{\kappa_i}} G_{tot} \tag{32}$$

and $\beta_i = \tilde{G}_i / G_i$.

A special case of noise scaling is *power scaling* in which all the multiplying factors β_i take the same value β and, hence, all capacitors and transconductors of the filter core are scaled by β. In this case, the total output noise mean-squared value of the filter is transformed according to $\overline{\tilde{U}^2_{no}} = \overline{U^2_{no}}/\beta$, without affecting the distortion behaviour.

Another possibility for filter scaling relies on multiplying column matrices instead of rows. Assuming that the column factors are γ_j, for $j = 1, \ldots, n$, and applying the transformation,

$$\begin{aligned} \tilde{\mathbf{E}} &= \mathbf{E}\mathbf{Diag}(\{\gamma_j\}) \\ \tilde{\mathbf{A}} &= \mathbf{A}\mathbf{Diag}(\{\gamma_j\}) \\ \tilde{\mathbf{C}} &= \mathbf{C}\mathbf{Diag}(\{\gamma_j\}) \end{aligned} \tag{33}$$

then, it can be derived by simple matrix algebra that the transfer functions $\mathbf{F}$ and $\mathbf{G}$ become,

$$\begin{aligned} \tilde{\mathbf{F}} &= (s\tilde{\mathbf{E}} - \tilde{\mathbf{A}})^{-1}\mathbf{B} = \mathbf{Diag}(\{1/\gamma_j\})\mathbf{F} \\ \tilde{\mathbf{G}} &= \tilde{\mathbf{C}}(s\tilde{\mathbf{E}} - \tilde{\mathbf{A}})^{-1} = \mathbf{G} \end{aligned} \tag{34}$$

and, thereafter, that $\tilde{H}(s) = H(s)$. Given that matrix $\mathbf{G}$ remains unaltered after scaling, $\tilde{w}_{ii} = w_{ii}$, and, therefore, the noise contributed to the output from the *i-th* integration node in the scaled filter becomes

$$\overline{\tilde{U}^2_{no,i}} = 2kT\xi w_{ii}\tilde{G}_i = 2kT\xi w_{ii}\left(|b_i| + \sum_j \gamma_j |a_{ij}|\right) \tag{35}$$

On the other hand, the transformation in (33) affects the amplitude level of the voltages at the internal nodes of the filter and, therefore, modifies its distortion behaviour. This can be clearly observed by replacing (33) and (34) into (25). Thus, for instance, the expression for the third-order harmonic distortion becomes

$$\tilde{HD}_3(\omega) = \frac{1}{4}\left|\frac{\mathbf{G}(3\omega)(\mathbf{A}\mathbf{Diag}(\{1/\gamma_j^2\})\mathbf{F}^{(3)}(\omega) + \mathbf{B}_G)}{H(\omega)}\right|\rho^2 \tag{36}$$

from where it can be inferred that the distortion contribution from the *j*-th integration node can be changed modifying γ_j. For this reason, this kind of scaling has been referred to as *distortion scaling*.

5.1 Scaling using unitary transconductors

In the practice, most of the designers use transconductors multiple of a unitary one. This fact limits the value of the coefficients used in the scaling process but makes the design faster and less sensitive to mismatch. To use unitary transconductors β_i and γ_i must be restricted to rational numbers, thus if we denote $\beta_i = k_i/l_i$ and $\gamma_i = m_i/n_i$ with

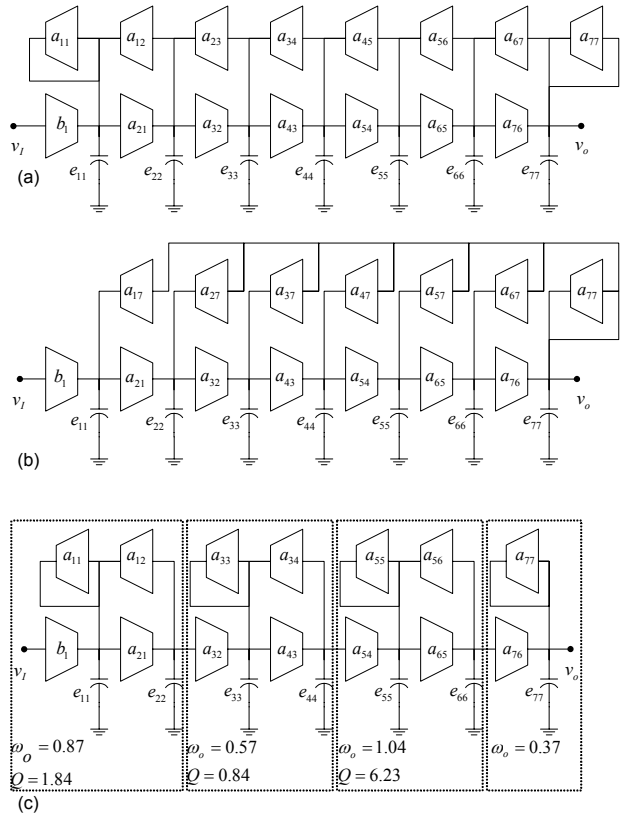

Fig. 3. Differents structures of a seventh order low-pass filter. (a) Lc ladder emulation, (b) FLF and (c) Cascade conection

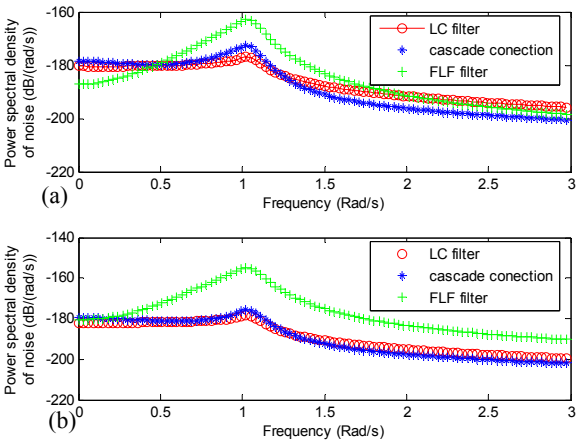

Fig. 4. Power spectral density of noise of the different structures (a) before and (b) after the optimization

k_i, l_i, m_i and n_i integer numbers, each a_{ij} and e_{ij} are transformed into $\tilde{a}_{ij}, \tilde{e}_{ij} = (k_i m_j)/(l_i n_j) \times (a_{ij}, e_{ij})$. To transform $\tilde{a}_{ij}$ into a integer number we must multiply it by the least common multiple of the non-zero values of matrix $\mathbf{A}$. Then $\tilde{a}_{ij}$ is transformed into $\hat{a}_{ij} = p_{ij}$ with p_{ij} integer. To get a filter with the minimum possible transconductors we divide the matrix $\hat{\mathbf{A}}$ by the greatest common divider of the non-zero values of the matrix $\hat{\mathbf{A}}$. In case of filters with floating capacitors, as e_{ij} must be equal to e_{ji} the following relation between the scaling coefficients must be satisfied

$$\frac{k_i m_j}{l_i n_j} = \frac{k_j m_i}{l_j n_i} \tag{37}$$

This condition limits the scaling possibilities of such filters. Scaling coefficients described above can be used in a optimization algorithm to improve some characteristics of the filters as distortion noise, DR or area.

6. Comparison of different structures

Taking into account noise and distortion in G_m-C filters description explained at Sec. 3 and Sec. 4 and the scaling process explained at Sec. 5, different kinds of structures can be compared. In this section a LC ladder emulation (which gives the leap-frog topology), a cascade connection of biquadratic section and the inverse follow the leader structure (**FLF**) of a seventh order low-pass Chebyshev filter using the G_m-C technique will be compared. The filter has a cut-off frequency of 1 rad/s and less than 0.1 dB ripple in the pass-band. These structures are shown in Fig.3. To improve the DR of the filter we have used a simulated annealing algorithm to minimize the following cost function

$$\cos t = \frac{DR_o}{DR} + 0,05\frac{n_{trans}}{n_{trans_o}} \tag{38}$$

where n_{trans} is the total number of transconductors of the filter and the sub-index o denotes the initial state. This cost function tries to maximize the DR without increasing the total number of transconductors in order to facilitate the interconnection between them. In the design of the filter using cascade connection of biquadratic sections all the possible permutations of the sections have been taking into account. The best location of the sections is shown in Fig.3(c). Fig.4 shows the power spectral density of noise of the filters for the three structures before and after the optimization process. It has been considered $\xi = 1$ and a total power consumption of $1W$. The current efficiency of the transconductor (Γ) defined as the ratio between the transconductance and the total current consumption of the transconductor has been set to $\Gamma = 1V^{-1}$ and the power supply to $1V$. Fig.5 shows the intermodulation versus the frequency of the structures for two tones of $A = 1V$ and third order non-linearity coefficient for the transconductor of $h_3 = 0,01V^{-2}$. Table 1 shows the number of unitary transconductors in the structures and summarizes the main characteristics of the filter. The fact that one structure has more transconductors than another does not implies that its power consumption is bigger since the value of the unitary transconductor is smaller. Thus, all the characteristics of the table are normalized to a power of 1 W. In the same way, the coefficients a_{ij} and e_{ij} are normalized to the unitary transconductor G_u. To calculate the DR it has been supposed that the worst case of acceptable IM_3 is -40 dB. As shows Table 1, the best DR is achieve using the structure

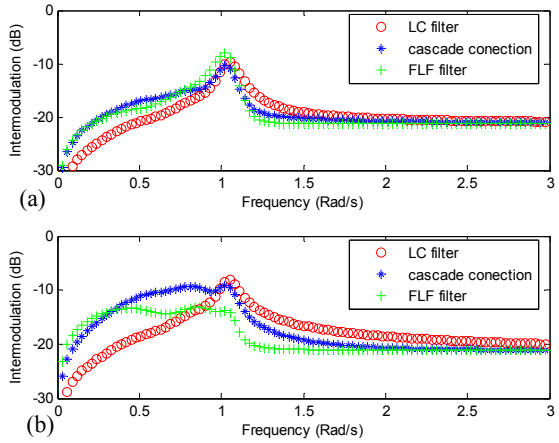

Fig. 5. IM_3 versus frequency of the filter for two tones of 1 V of amplitude for the structures (a) before and (b) after the optimization

which emulate the LC ladder, followed by the cascade connections of biquadratic sections. This table also shows that the DR of the FLF structure is 14 dB worst than the LC ladder emulation one. This fact implies that to achieve the same DR, FLF structure would need 25 times more power than LC emulation one (Power increases a factor two when DR improves 3 dB).

7. Conclusions

This paper presents techniques to describe and to evaluate the noise and distortion of continuous time filters using dot-matrix description. Using these techniques a comparison between the DR for a given power consumption of the most commonly used structures to make G_m-C filters has been made. It shows that for a seventh order, low-pass chebyshev filter the best DR is achieved for the LC ladder emulation. The DR using cascade connection is very close to the LC ladder one but is 14 dB worse in the FLF structure. This fact implies that this structure would consume 25 times more power than the lc ladder emulation one to achieve the same DR and hence should be avoided in low power designs.

Table 1: Number of unitary transconductors and main characteristic of the filter using different structures. The first column is for the non-optimized filter and the second one for the optimized one

LC emulation			Cascade connection			FLF structure		
b_1	1	2	b_1	10	8	b_1	1	1
a_{11}	-1	-1	a_{11}	-10	-8			
a_{21}	2	2	a_{21}	13	13	a_{21}	3	3
a_{32}	1	3	a_{32}	16	6	a_{32}	8	8
a_{43}	2	4	a_{43}	17	12	a_{43}	13	18
a_{54}	2	4	a_{54}	18	5	a_{54}	15	20
a_{65}	2	3	a_{65}	26	26	a_{65}	15	40
a_{76}	2	3	a_{76}	21	15	a_{76}	8	21
a_{12}	-1	-2	a_{12}	-10	-8	a_{17}	-1	-2
a_{23}	-2	-4	a_{33}	-8	-6	a_{27}	-3	-6
a_{34}	-1	-3	a_{34}	-24	-3	a_{37}	-8	-12
a_{45}	-2	-3	a_{55}	-5	-5	a_{47}	-13	-18
a_{56}	-2	-2	a_{56}	-36	-25	a_{57}	-15	-20
a_{67}	-1	-2	a_{77}	-7	-6	a_{67}	-15	-30
a_{77}	-1	-3				a_{77}	-8	-14
e_{11}	1.18	1.18	e_{11}	14.7	17.0	e_{11}	5.48	5.48
e_{22}	2.85	5.69	e_{22}	26.2	8.11	e_{22}	7.91	10.6
e_{33}	2.10	6.29	e_{33}	17.0	8.84	e_{33}	14.6	21.9
e_{44}	3.15	6.29	e_{44}	31.8	12.3	e_{44}	15.2	21.1
e_{55}	4.20	6.29	e_{55}	29.8	29.8	e_{55}	15.1	26.8
e_{66}	2.84	2.84	e_{66}	28.7	19.9	e_{66}	7.98	23.9
e_{77}	1.18	3.54	e_{77}	18.6	15.9	e_{77}	4.72	8.26
$\overline{U_{no}^2}$ (nV^2rms)	**1.0**	**0.64**		**1.5**	**0.90**		**44**	**49**
DR (dB)	**169.7**	**170.1**		**168.7**	**169.6**		**151.4**	**156.2**
n_{trans}	**23**	**41**		**221**	**146**		**126**	**214**
G_u (mA/V)	**43.5**	**24.4**		**4.52**	**6.85**		**7.94**	**4.67**

References

[1] S. Koziel, R. Schaumann, and X. Haiqiao, "Analysis and optimization of noise in continuous-time OTA-C filters," *Circuits and Systems I: Regular Papers, IEEE Transactions on*, vol. 52, pp. 1086-1094, 2005.

[2] Behbahani, F., W. Tan, et al. (2000). "A broad-band tunable CMOS channel-select filter for a low-IF wireless receiver." Solid-State Circuits, IEEE Journal of 35(4): 476-489.

[3] Gopinathan, V., M. Tarsia, et al. (1999). "Design considerations and implementation of a programmable high-frequency continuous-time filter and variable-gain amplifier in submicrometer CMOS." Solid-State Circuits, IEEE Journal of 34(12): 1698-1707.

[4] G. Groenewold, "The design of high dynamic range continuous-time integratable bandpass filters," *Circuits and Systems, IEEE Transactions on*, vol. 38, pp. 838-852, 1991.

[5] Sun, Y. and J. K. Fidler (1997). "Structure generation and design of multiple loop feedback OTA-grounded capacitor filters." Circuits and Systems I: Fundamental Theory and Applications, IEEE Transactions on 44(1): 1-11.

[6] V. Mehrmann and T. Stykel, "Balanced truncation model reduction for large-scale systems in descriptor form". Dimension Reduction of Large-Scale Systems, *Lecture Notes in Computational Science and Engineering*, vol. 45, pp. 83-115. Springer-Verlag, Berlin/ Heidelberg, 2005.

[7] M. Schetzen, *The Volterra and Wiener theories of nonlinear systems*, Malabar, Florida, Krieger, 1980.

[8] Y. Palaskas and Y. Tsividis, "Dynamic range optimization of weakly nonlinear, fully balanced, Gm-C filters with power dissipation constraints," *Circuits and Systems II: Analog and Digital Signal Processing, IEEE Transactions on*, vol. 50, pp. 714-727, 2003.